

NASA Technical Memorandum 4047

**Theoretical Derivation and
Calibration Technique of
a Hemispherical-Tipped,
Five-Hole Probe**

Scott O. Kjelgaard
Langley Research Center
Hampton, Virginia



National Aeronautics
and Space Administration

**Scientific and Technical
Information Division**

1988

Summary

A technique is presented for the calibration of a hemispherical-tipped, five-hole probe having a 0.125-in. diameter. Equations are derived from the potential flow over a sphere relating the flow angle and velocity to pressure differentials measured by the probe. The technique for acquiring the calibration data and the technique for calculating the calibration coefficients are presented. The accuracy of the probe in both the uniform calibration flow field and the nonuniform flow field over a 75°-swept delta wing is discussed.

Introduction

The measurement of flow field quantities, such as flow velocity and angularity, has been conducted with the use of pressure probes with great success for many years. Through the years, a variety of pressure probe designs and calibration techniques have been developed. (See ref. 1.) The hemispherical-tipped, five-hole probe is a good probe for the measurement of flow velocity and angularity in low-speed flows because of its high sensitivity to flow angle and its insensitivity to Reynolds number based on probe diameter R_d (i.e., $2 \times 10^3 < R_d < 150 \times 10^3$).

This report details the theoretical derivation of calibration equations and the calibration technique for a hemispherical-tipped, five-hole probe having a 0.125-in. diameter. This probe is used in the Langley Basic Aerodynamics Research Tunnel (BART). The potential flow over a sphere is used to derive equations relating total-flow angle, roll angle, and velocity to pressure differences. These equations are generalized and experimental data are then fit, in a least-squares sense, to obtain the calibration coefficients used to measure the flow over the 75°-swept delta wing. This calibration technique is an extension of the method used in reference 2, and the theoretical derivation of the calibration equations is also based on reference 2.

Symbols

$A, B, C, D,$ E, F, G	calibration constants defined by equations (19), (20), (21), and (22)
b	local span of 75°-swept delta wing, ft
D_p	particle diameter, ft
d	probe diameter, ft
f_i	dimensionless pressure on port i defined as $(p_i - p_s)/q$

L	root chord of 75°-swept delta wing (1.866 ft)
N_{St}	Stokes number, $\frac{1}{18} \frac{\rho_p}{\rho_a} \frac{U_s D_p}{\nu} \frac{D_p}{r}$
p_i	pressure at port i , lb/ft ²
p_s	static pressure of flow, lb/ft ²
Δp_α	difference in pressure between pitch ports, lb/ft ²
Δp_β	difference in pressure between yaw ports, lb/ft ²
q	dynamic pressure of flow, $\frac{1}{2} \rho U_\infty^2$, lb/ft ²
q_p	quantity defined by equation (15), lb/ft ²
R	Reynolds number based on root chord, VL/ν
R_d	Reynolds number based on probe diameter, Vd/ν
r	vortex core radius, ft
rms	root mean square
S_α	sensitivity of probe to pitch, $\frac{\text{lb}}{\text{ft}^2}/\text{deg}$
S_β	sensitivity of probe to yaw, $\frac{\text{lb}}{\text{ft}^2}/\text{deg}$
U_s	swirl velocity near vortex core, ft/sec
U_∞	free-stream velocity of flow, ft/sec
u, v, w	streamwise, lateral, and vertical velocity components, respectively, in body axis system, ft/sec
V	velocity of flow at surface of sphere, ft/sec
x, y, z	distance from coordinate origin in tunnel axis system, ft
α	pitch angle of total-pressure port to stagnation point, deg
α_0	pitch error due to manufacturing, deg
β	yaw angle of total-pressure port to stagnation point, deg
β_0	yaw error due to manufacturing, deg

θ	total angle of total-pressure port to stagnation point, deg
θ_i	angle between the i th port and stagnation point, deg
θ_0	total angle where q_p becomes zero, singularity point of equation (19), deg
ν	kinematic viscosity, ft ² /sec
ρ	density, slugs/ft ³
ϕ	roll angle at total-pressure port from lower α port to stagnation point, deg
ϕ_0	fixed roll-angle error between probe calculation and sting, deg
ψ	yaw angle of probe, deg
$\psi_{0,pitch}$	misalignment in pitch between probe and free stream, deg
$\psi_{0,yaw}$	misalignment in yaw between probe and free stream, deg

Subscripts:

a	air
meas	measured
p	particle

Calibration Technique

The probe to be calibrated is a yaw-pitch probe with a total-pressure port at the forward point of a hemispherical tip and a ring of six interconnected static ports approximately eight probe diameters from the tip. Details of the probe are presented in figure 1. To measure the angle of the velocity vector, four ports are placed at approximately 45° to the total-pressure port in the directions of yaw and pitch. The total-pressure port and static-pressure port are numbered ports 1 and 2, respectively. (See fig. 2.) When the probe is lined up with the local velocity vector, the difference between these pressures gives the standard incompressible measurement of the dynamic pressure. When looking upwind, the right and left ports are called the β ports and are labeled 3 and 4, respectively. These will give the angle of yaw, which is the angle β . The top and bottom ports are called the α ports and are labeled 5 and 6, respectively. These will give the angle of pitch, which is the angle α .

To specify the orientation of the velocity vector with respect to the probe, the usual coordinates are

the angles α and β , which are rotated about the y - and z -axes of the probe as shown in figure 2. For a complete solution of the calibration problem to large angles, it is more convenient to use the angles θ and ϕ . Since the pressures on the hemispherical tip are assumed to be symmetrical about the stagnation point, the significant angle is the total angle θ that the probe makes with the velocity vector. To specify the direction of the velocity vector relative to the probe, a polar angle ϕ is taken about the probe and referenced to the lower α port. Spherical trigonometry yields the following conversion between the two coordinate systems:

$$\tan \alpha = \tan \theta \cos \phi \quad (1a)$$

$$\sin \beta = \sin \theta \sin \phi \quad (1b)$$

$$\cos \theta = \cos \alpha \cos \beta \quad (1c)$$

$$\tan \phi = \tan \beta / \sin \alpha \quad (1d)$$

Calibration Based on the Potential Flow Over a Sphere

This calibration technique closely follows the method described in reference 2. The pressure on a sphere is a function only of the total angle θ from the stagnation point. A nondimensional quantity f_i may be defined as the pressure at port i (p_i) minus the static pressure (p_s), divided by the dynamic pressure (q):

$$f_i(\theta_i) = \frac{p_i - p_s}{q} \quad (2)$$

This quantity can be determined theoretically by using the potential-flow theory for uniform flow over a sphere. If axisymmetric flow is assumed, the superposition of a free stream and a doublet flow gives the velocity on the surface of the sphere as

$$V(\theta) = \frac{3}{2} U_\infty \sin \theta \quad (3)$$

Bernoulli's equation is then used to obtain the pressure distribution on the sphere as

$$p_i + \frac{1}{2} \rho V^2 = p_s + \frac{1}{2} \rho U_\infty^2 \quad (4)$$

By using this equation and the definition of f_i , one obtains

$$f_i(\theta_i) = \frac{9}{4} \cos^2 \theta_i - \frac{5}{4} \quad (5)$$

The most important quantities are the differences in pressure between the two α ports and the two β ports. These are labeled Δp_α and Δp_β , respectively, with the convention that they are positive in the

α - and β -directions. From the definition of f_i , the following relations are obtained:

$$\Delta p_\alpha = q(f_6 - f_5) \quad (6)$$

$$\Delta p_\beta = q(f_3 - f_4) \quad (7)$$

By using the functional form of f_i , one obtains the relations

$$\Delta p_\alpha = \frac{9}{4}q(\cos^2 \theta_6 - \cos^2 \theta_5) \quad (8)$$

$$\Delta p_\beta = \frac{9}{4}q(\cos^2 \theta_3 - \cos^2 \theta_4) \quad (9)$$

These relations can be converted to functions of θ and ϕ by reference to figure 2. The law of cosines for spherical triangles yields

$$\cos \theta_6 = \cos \theta \cos 45^\circ + \sin \theta \sin 45^\circ \cos \phi \quad (10a)$$

$$\cos \theta_5 = \cos \theta \cos 45^\circ - \sin \theta \sin 45^\circ \cos \phi \quad (10b)$$

$$\cos \theta_4 = \cos \theta \cos 45^\circ - \sin \theta \sin 45^\circ \cos \phi \quad (10c)$$

$$\cos \theta_3 = \cos \theta \cos 45^\circ + \sin \theta \sin 45^\circ \cos \phi \quad (10d)$$

By substituting these equations into the equations for Δp_α (eq. (8)) and Δp_β (eq. (9)), one obtains

$$\Delta p_\alpha = \frac{9}{4}q \sin 2\theta \cos \phi \quad (11)$$

$$\Delta p_\beta = \frac{9}{4}q \sin 2\theta \sin \phi \quad (12)$$

The dependence on θ and ϕ can be separated by taking the ratio and the square root of the sum of the squares of these two equations:

$$\frac{\Delta p_\beta}{\Delta p_\alpha} = \tan \phi \quad (13)$$

$$(\Delta p_\alpha^2 + \Delta p_\beta^2)^{1/2} = \frac{9}{4}q \sin 2\theta \quad (14)$$

The square-root quantity may be nondimensionalized by dividing by the quantity q_p , defined as the pressure on port 1 minus the average of the pressures on the four angle ports. This relation can be written in terms of f_i as

$$q_p = q \left[f_1 - \frac{1}{4}(f_3 + f_4 + f_5 + f_6) \right] \quad (15)$$

Substituting equations (5) and (10) into (15) reduces equation (15) to

$$q_p = q \left(\frac{27}{32} \cos 2\theta + \frac{9}{32} \right) \quad (16)$$

Substituting equation (16) into equation (14) yields

$$\frac{(\Delta p_\alpha^2 + \Delta p_\beta^2)^{1/2}}{q_p} = \frac{\frac{9}{4} \sin 2\theta}{\frac{27}{32} \cos 2\theta + \frac{9}{32}} \quad (17)$$

It should be noted that this has a singularity at 54.7° . The technique given here does not use the measurements made on the static-pressure ports, which can have significant errors at large angles to the velocity. However, once the dynamic pressure q and the total angle θ are known, the static pressure can be calculated from the quantity f_1 by using the following formula:

$$p_1 - p_s = q \left(\frac{9}{4} \cos^2 \theta - \frac{5}{4} \right) \quad (18)$$

Equations (13), (16), (17), and (18) determine the primary quantities from which the angles θ and ϕ and the pressures q and p_s can be found.

Generalization of Calibration Technique

For a number of reasons, the potential-flow calibration may not be satisfactory for a given yaw-pitch probe. The decrease in pressures with θ given by the potential-flow theory is ideal for a sphere only while the probe is a hemispherical-tipped cylinder, and thus the decreased pressures differ from experimental values at large distances from the stagnation point. The placement of the ports may be in error because of manufacturing problems. This means that there will be fixed errors in the α - and β -directions, in the rotation angle ϕ , and in the sums and differences of the pressures on the α and β ports. For these reasons the theoretical calibration is generalized to include some experimentally determined parameters. While maintaining the same form, the constants of the θ dependence are made arbitrary so that equations (16), (17), and (18) are generalized to become

$$\frac{(\Delta p_\alpha^2 + \Delta p_\beta^2)^{1/2}}{q_p} = A \frac{\sin 2\theta}{\cos 2\theta - \cos 2\theta_0} \quad (19)$$

$$q_p = q [C(\cos 2\theta - \cos 2\theta_0) + D(\cos \theta - \cos \theta_0)] \quad (20)$$

$$p_1 - p_s = q(E \cos^2 \theta + F \cos \theta + G) \quad (21)$$

The constant θ_0 is the singularity point of equation (19) and must be the same for equation (20) to determine correct values for q . The calculation for ϕ (eq. (13)) is made arbitrary by the subtraction of a constant ϕ_0 and the multiplication by a constant B as follows:

$$\frac{B \Delta p_\beta}{\Delta p_\alpha} = \tan(\phi - \phi_0) \quad (22)$$

It should be noted that the constants B and ϕ_0 do not appear in the generalization of reference 2.

Determination of Calibration Constants

The experimental technique for acquiring the five-hole probe calibration data and the calculation of the calibration constants are described in this section. The 0.125-in-diameter five-hole probe was mounted in the test section of the Langley Basic Aerodynamics Research Tunnel on a C-strut so that the probe tip was always positioned at the same location when the probe was yawed. Pressure data were obtained using an electronic scanning pressure system with ± 1 lb/in² transducers. Four sets of calibration data were obtained at eight free-stream velocities. A set of calibration data was obtained by yawing the probe between -90° and 90° in 1° increments. The four data sets were obtained by rolling the probe through 90° increments. (Positive roll is counterclockwise when looking downstream at the probe tip.) A typical data set is presented in figure 3 for a free-stream velocity of 160 ft/sec and a roll of 0° . These data sets were then used to calculate the calibration coefficients. The procedure used to calculate the calibration coefficients involved six computer codes and is described below.

Before the discussion of the methods used to calculate the probe errors and calibration coefficients, a few comments about the experimental procedure are necessary. When the probe is rolled 0° or 180° , the data acquired are for the calibration of the β ports (ports 3 and 4). When the probe is rolled 90° or 270° , the data acquired are for the calibration of the α ports (ports 5 and 6). The probe is always yawed in the same direction; therefore, when the probe is rolled 0° ,

$$\beta = +\psi$$

when rolled 90° ,

$$\alpha = -\psi$$

when rolled 180° ,

$$\beta = -\psi$$

and when rolled 270° ,

$$\alpha = +\psi$$

There are two sets of values for the constants θ_0 , ϕ_0 , A , B , C , D , E , F , and G . One set is derived for the α ports and the other set for the β ports. Each set of constants is used to calculate a value of θ and ϕ from the pressures measured by the five-hole probe. These two independent measures of θ and ϕ are converted into α and β and then are combined by using a cosine weighting function based on the roll angle ϕ . The final values of θ and ϕ are obtained using equations (1c) and (1d), respectively.

Step 1—Calculation of probe manufacturing errors and misalignment errors between the probe and the free stream. The first step in the probe calibration procedure is the determination of the probe manufacturing errors and the misalignment errors between the probe and the free stream. These errors are defined as α_0 and β_0 (the errors caused by improper placement of the pressure orifices) and $\psi_{0,yaw}$ and $\psi_{0,pitch}$ (the misalignment errors of the probe with the free stream). Roll data that are 180° out of phase are used to calculate these errors.

To understand how the misalignment error of the probe with the free stream in yaw ($\psi_{0,yaw}$) is calculated, assume that the probe is made perfectly (i.e., no probe error) and that we are looking at data for the β ports (rolls of 0° and 180°). If the probe is misaligned in yaw by some positive increment, then the probe reading Δp_β at zero yaw will be negative for the roll of 0° and positive for the roll of 180° (fig. 4(a)). The probe will have the same magnitude of sensitivity to flow angle in either roll; however, the sign of the sensitivity will be the opposite for the roll of 180° . Plotting the two roll data sets on the same plot yields figure 4(b), and the probe misalignment error is found at the intersection of the two curves. One should note that this error should be the same for both the β calibration data sets and the α calibration data sets because of the method of obtaining the calibration data.

Probe error due to manufacturing is found by a similar method. Assume that the probe is perfectly aligned with the free-stream direction, but the β ports have been incorrectly placed as illustrated in figure 5(a). For the roll of 0° , the five-hole probe would measure some flow angle at 0° yaw ($+\Delta p_\beta$). For the roll of 180° , the five-hole probe would measure the same value of $+\Delta p_\beta$. Once again the sensitivity of the probe to flow angle would have the same magnitude but would differ in sign for the two roll cases. If one uses this information, a figure can be constructed that allows the probe manufacturing error to be calculated (fig. 5(b)). This technique is also used for the α ports.

Because the probe is not rotated in pitch, the only method for calculating the misalignment of the probe in pitch is by using the flow angle predicted by the probe and the probe error due to manufacturing. Figure 6 presents sketches that help in the understanding of this pitch misalignment. The measured Δp_α is a function of the error in manufacturing of the α ports and the misalignment of the probe with the free stream in pitch so that

$$\psi_{0,\text{pitch}} = [(\Delta p_\alpha/q)/S_\alpha] - \alpha_0$$

for the rolls of 0° and 180° , where S_α is determined by the slope of the calibration data. (Determination of S_β is demonstrated in fig. 5.)

Figure 7 presents the results for rolls of 0° and 180° for the five-hole probe with a free-stream velocity of 160 ft/sec and shows the combined effect of probe error due to manufacturing and misalignment. These errors can be measured directly off the plot; however, the code used for step 1 of the probe calibration calculates the errors by fitting a least-squares linear fit to the data in the yaw range from -12° to 12° and calculates the intersection of the two curves with each other and with the horizontal axis. These intersections yield the information required to deduce the probe manufacturing and misalignment errors. One last point, because the probe is rolled, the combination of probe errors due to manufacturing and misalignment with free stream is different for each roll angle to correct the calibration data properly. Thus, for a roll of 0° ,

$$\beta = \psi - \psi_{0,\text{yaw}} - \beta_0$$

$$\alpha = -\psi_{0,\text{pitch}} - \alpha_0$$

for a roll of 90° ,

$$\beta = -\psi_{0,\text{pitch}} - \beta_0$$

$$\alpha = -(\psi - \psi_{0,\text{yaw}} + \alpha_0)$$

for a roll of 180° ,

$$\beta = -(\psi - \psi_{0,\text{yaw}} + \beta_0)$$

$$\alpha = -\psi_{0,\text{pitch}} + \alpha_0$$

and for a roll of 270° ,

$$\beta = -\psi_{0,\text{pitch}} + \beta_0$$

$$\alpha = \psi - \psi_{0,\text{yaw}} - \alpha_0$$

Step 2—Calculation of calibration coefficients θ_0 and A . Once the probe manufacturing errors and the probe misalignment with the free stream are subtracted from the calibration data, the calibration coefficients θ_0 and A are found by fitting the calibration data to equation (19). Although yaw data are obtained between -90° and 90° , only yaw data between -45° and 45° are used for the curve fit. The data are fit in a least-squares sense by using the differential correction method detailed in reference 3. It is assumed for the first iteration that B and ϕ_0 are equal to their theoretical values (1 and 0, respectively).

Step 3—Calculation of calibration coefficients ϕ_0 and B . Once θ_0 and A are obtained from step 2, the calibration coefficients ϕ_0 and B are found by fitting the calibration data to equation (22) in a least-squares sense by using the differential correction method. Once these constants have been found, they are used in the step 2 calculations to yield a better fit for θ_0 and A . Steps 2 and 3 are iterated until the constants θ_0 , A , B , and ϕ_0 have converged (usually requiring three iterations). The iteration technique is required by the software used to calculate the yaw and pitch from the differential pressures measured by the five-hole probe. (See the appendix.)

Step 4—Calculation of calibration coefficients C and D . Once the constants θ_0 , A , B , and ϕ_0 have converged, they are used to calculate the calibration coefficients C and D . These coefficients relate the pressures measured at the tip of the probe to the local dynamic pressure of the flow and are found in a manner similar to the others. The calibration data are fit in a least-squares sense to equation (20) by using the differential correction method.

Step 5—Calculation of calibration coefficients E , F , and G . The last step in the probe calibration is the calculation of the calibration coefficients E , F , and G . These coefficients relate the pressures measured on the probe tip to the static pressure in the flow. The best-fit values for the calibration coefficients θ_0 , ϕ_0 , A , B , C , and D are used while the calibration data are fit, in a least-squares sense, to equation (21) by using the differential correction technique mentioned previously.

Technique for Measuring Unknown Flow Velocity and Angularity

Once the calibration coefficients are obtained, their dependence on free-stream velocity (Reynolds

number) can be assessed. Figure 8 presents the calibration coefficients θ_0 , ϕ_0 , A , B , C , and D as a function of free-stream velocity. (This set of calibration data did not allow for the calibration of the static pressure.) A third-order polynomial curve fit was made to each of the calibration coefficients, and these polynomials were incorporated into the subroutine that calculates the flow angularity and velocity from the measured pressures. This subroutine is presented in the appendix. The flow angularity and velocity were found in an iterative manner. The free-stream velocity is used to calculate the first set of calibration coefficients, and on the subsequent iterations the velocity predicted by the five-hole probe is used to calculate the calibration coefficients. The flow angularity and velocity are found when the velocity predicted by the probe has converged to one value.

Accuracy of Five-Hole Probe

The measured flow angle and velocity have been compared with the known values of flow angle and velocity for the calibration data. The probe error was calculated by taking the root mean square (rms) of the difference between the known and the measured flow angle and velocity. These rms errors are presented as the solid lines in figure 9. The figures indicate that the probe measurements for $\theta < 50^\circ$ are as follows: the pitch angle α within 0.5° , the yaw angle β within 1.5° , and the dynamic pressure q within 0.02 lb/ft^2 . Figure 9 also presents the effect of Reynolds number for the range of Reynolds number that the probe was calibrated over. These data (the dashed lines in fig. 9) were found by taking the calibration constants for the highest Reynolds number and applying them to the data acquired for the lowest Reynolds number and vice versa. These data indicate little effect due to Reynolds number in the measurements of α and β ; however, the error in the measurement of the dynamic pressure increases by a factor of 3.

These characteristics were measured with a uniform onset flow. When the probe is introduced into the flow over a model, the flow field seen by the probe is no longer uniform. The gradients in the flow field can affect the accuracy of the probe and the probe may disturb the flow field. To help understand the magnitude of the errors caused by the five-hole probe in a nonuniform flow field, a comparison has been conducted (ref. 4) between flow field data obtained over a 75° -swept delta wing with the five-hole probe and data obtained by a three-component laser Doppler velocimeter (LDV). The LDV is capable of obtaining accurate velocity measurements in flow fields with reverse flows, large shear gradients, and velocity fluctuations. The BART LDV

system is a three-color, orthogonal, cross-fringe configuration with the receiving optics package mounted 90° off-axis. The 514.5-, 496.5-, and 476.5-nm wavelengths are used to measure the lateral (v), stream-wise (u), and vertical (w) velocity components, respectively. Bragg cells are used to provide directional measurement capability in all three velocity components. The sample volume is spherical in shape and has been calculated to be approximately $150 \mu\text{m}$ in diameter. The optics and laser move as a unit on a traversing system that provides 1 m of travel, with $10 \mu\text{m}$ of resolution, in all three axes.

The flow field was seeded with $0.8\text{-}\mu\text{m}$ polystyrene latex microspheres. The seed particles were suspended in a mixture of alcohol and water and were injected into the flow upstream of the honeycomb by using an atomizing spray nozzle. Typically, 500 to 4096 velocity samples were obtained at each measurement location in the flow field. The actual number of samples depended on the particular location in the flow field and the particle seeding rate.

The ability of a particle to track the streamlines in the flow field, and thus the accuracy of the LDV, is directly related to the size of the particle. Theoretical predictions of particle trajectories in various flows were reported in references 5 through 7. Dring and Suo (ref. 5) concluded that the particle trajectory in a free-vortex swirling flow is governed primarily by the Stokes number (N_{St}); and when the Stokes number is less than 0.01, the particle will follow the circular streamlines of the free vortex.

The $0.8\text{-}\mu\text{m}$ particles used during this test have a density ρ_p of $2.03727 \text{ slugs/ft}^3$. The Stokes number for the particles is 0.007, based on the radius and the swirl velocity at the edge of the vortex core. The numerical procedure described by Dring (ref. 7) was used to predict the particle trajectories for the vortices that were measured during this investigation. The predictions show that the particles used during this test will follow the streamlines of the vortex with an accuracy of about 1 percent.

The velocity surveys were made over a 75° -swept delta wing at an angle of attack of 20.5° and a Reynolds number of 1×10^6 based on the root chord. These velocity surveys are presented in figure 10. The differences in the u , v , and w components of the flow field are presented in figure 11. In the core of the vortex the five-hole probe has errors in the u , v , and w components of velocity of 25, 17, and 35 percent, respectively. The errors were calculated assuming that the LDV measurements were the reference. The

equation used to calculate the u -component error is

$$u_{\text{error}} = 100 \frac{u_{\text{LDV}} - u_{\text{FH}}}{(u_{\text{LDV}}^2 + v_{\text{LDV}}^2 + w_{\text{LDV}}^2)^{1/2}}$$

where the subscript FH denotes the five-hole probe. The errors in v and w are calculated in a similar fashion.

Figure 12 presents the gradients in the v and w components of velocity measured by the five-hole probe for the same data set. A comparison of figures 11 and 12 shows that the probe does a reasonable job of measuring the flow field quantities in regions of low gradients (with a probe error less than 5 percent when the velocity gradient is less than $800 \frac{\text{ft}}{\text{sec}}/\text{ft}$). However, in the vortex core, very high gradients ($> 3000 \frac{\text{ft}}{\text{sec}}/\text{ft}$) yield differences of more than 20 percent between the two measurement techniques.

Concluding Remarks

A technique has been presented for the calibration of a hemispherical-tipped, five-hole probe with a 0.125-in. diameter. Equations were derived from the potential flow over a sphere relating the flow angle and velocity to pressure differentials measured by the probe. Four sets of calibration data were acquired at eight free-stream velocities. A set of calibration data was obtained by yawing the probe between -90° and 90° in 1° increments. The four

data sets were obtained by rolling the probe through 90° increments. The calibration data are fit to the equations derived from the potential flow over a sphere to obtain the calibration coefficients, which are then used to convert measured pressures into flow angularity and velocity data.

To assess the ability of the five-hole probe to measure flow angularity and velocity, the known calibration data were compared with those measured by the five-hole probe. For the uniform flow field measured for the probe calibration, the probe measurements were as follows for a total angle of total-pressure port to stagnation point less than 50° : the pitch angle within 0.5° , the yaw angle within 1.5° , and the dynamic pressure within $0.02 \text{ lb}/\text{ft}^2$. For the non-uniform flow over a 75° -swept delta wing, comparisons between the five-hole probe and a three-component laser Doppler velocimeter showed that the probe performed a reasonable job of measuring the flow field quantities in regions of low gradients (with a probe error less than 5 percent when the velocity gradient is less than $800 \frac{\text{ft}}{\text{sec}}/\text{ft}$). However, in the vortex core, very high gradients ($> 3000 \frac{\text{ft}}{\text{sec}}/\text{ft}$) yielded differences of more than 20 percent between the two measurement techniques.

NASA Langley Research Center
Hampton, VA 23665-5225
September 20, 1988

Appendix

Listing of Five-Hole-Probe Subroutine

This subroutine is used to convert the pressures measured by the yaw-pitch probe into flow velocity and angularity.

```
      SUBROUTINE FIVE_HOLE(P,ALPHA,BETA,THETA,PHI,Q,PS,VEL_PREV)
C
C   FIVE_HOLE CONVERTS MEASURED PRESSURES INTO FLOW ANGLES
C   AND VELOCITY DATA USING THE CALIBRATION EQUATIONS DERIVED
C   IN APPENDIX A OF REFERENCE 2
C           SUBROUTINE WRITTEN BY KJELGAARD IN AUGUST 1986
C DESCRIPTION OF VARIABLES
C INPUT
C   P - ARRAY CONTAINING PRESSURES MEASURED BY 5-HOLE PROBE
C       P(1) CONTAINS PRESSURE AT PORT 1
C       P(2) CONTAINS PRESSURE AT PORT 2, ETC.
C OUTPUT
C   ALPHA - PITCH ANGLE MEASURED BY PROBE
C   BETA - YAW ANGLE MEASURED BY PROBE
C   THETA - TOTAL FLOW ANGLE MEASURED FROM PORT 1 TO STAGNATION
C           POINT
C   PHI - FLOW ROLL ANGLE MEASURED FROM LOWER ALPHA PORT TO
C           STAGNATION POINT
C   Q - DYNAMIC PRESSURE OF THE FLOW AT THE PROBE TIP
C   PS - STATIC PRESSURE MEASURED AT THE PROBE TIP
C   VEL_PREV - VELOCITY USED TO CALCULATE PROBE CONSTANTS
C
      REAL P(*)
      REAL ALPH(2),BET(2),THET(2),QT(2),PST(2)
      REAL A(2),THETA0(2),PHI0(2),B(2),C(2),D(2),E(2),F(2),G(2)
      EXTERNAL POLY
      DPA=P(6)-P(5)
      DPB=P(3)-P(4)
      QP=P(1)-.25*(P(3)+P(4)+P(5)+P(6))
      A1=SQRT(DPA**2+DPB**2)/QP
C-----
C   PROBE CONSTANTS
C-----
      A(1)=POLY(VEL_PREV,.13930,-2.5727E-3,1.43414E-5,0)
      A(2)=POLY(VEL_PREV,3.1607,-8.1927E-3,7.1750E-5,-1.8642E-7)
      THETA0(1)=POLY(VEL_PREV,55.595,-5.8621E-2,4.7727E-4,-1.1427E-6)
      THETA0(2)=POLY(VEL_PREV,57.134,-9.3249E-2,8.0274E-4,-2.0331E-6)
      B(1)=POLY(VEL_PREV,.31547,2.4019E-2,-2.0699E-4,5.5156E-7)
      B(2)=POLY(VEL_PREV,.67481,9.7006E-3,-7.1074E-5,1.4787E-7)
      PHI0(1)=POLY(VEL_PREV,-.48446,-4.9767E-2,4.5553E-4,-1.2265E-6)
      PHI0(2)=POLY(VEL_PREV,-4.2108,4.5463E-2,-2.7104E-4,4.4549E-7)
      C(1)=POLY(VEL_PREV,.25419,-1.6741E-3,9.3270E-6,-8.6405E-9)
      C(2)=POLY(VEL_PREV,.38568,-5.2703E-3,3.7782E-5,-8.2944E-8)
      D(1)=POLY(VEL_PREV,.74529,1.7064E-2,-1.1424E-4,2.2726E-7)
      D(2)=POLY(VEL_PREV,.23948,2.9862E-2,-2.1885E-4,5.0793E-7)
C
C   ITERATIVELY SOLVE FOR THETA
```

```

C
DO 1 I=1,2
  THET(I)=0.
  THSTEP=10.
C
C CALCULATE PHI
C
IF (DPA .EQ. 0) DPA=.00001
PHIM=ATAND(B(I)*DPB/DPA)
IF (DPA .LT. 0) PHIM=180.+PHIM
IF (PHIM .LT. 0) PHIM=PHIM+360.
PHIT=PHIM-PHI0(I)
A2=1
DO 2000 ILOOP=1,50
  IF (ILOOP .EQ.50) THEN
*   WRITE(6,(' TOO MANY ITERATIONS IN CALB'))
    THET(I)=.5*ACOSD(A(I)*SIND(2.*THETA0(I))/A1+
*     COSD(2.*THETA0(I)))
    GO TO 3170
  END IF
  THET(I)=THET(I) + THSTEP
  A3=COSD(2.*THET(I))-COSD(2.*THETA0(I))
  IF (A3.EQ.0.0) THEN
    WRITE(6,(' PROBLEM IN CALB'))
    WRITE(6,('4F10.5')) THET(I),THSTEP
    A3=1E-5
  END IF
  A2=A1-A(I)*SIND(2.*THET(I))/A3
  IF (A2 .LT. 0) THEN
    THET(I)=THET(I)-THSTEP
    THSTEP=THSTEP*.5
    GO TO 3160
  END IF
  IF (A2 .LE. .02) GO TO 3170
3160 CONTINUE
2000 CONTINUE
3170 ALPH(I)=ATAND(TAND(THET(I))*COSD(PHIT))
    BET(I)=ASIND(SIND(THET(I))*SIND(PHIT))
    QT(I)=QP/(C(I)*(COSD(2.*THET(I))-COSD(2.*THETA0(I)))+
*     D(I)*(COSD(THET(I))-COSD(THETA0(I))))
    PST(I)=P(1)-QT(I)*(E(I)*COSD(2.*THET(I))+F(I)*COSD(THET(I))
*     +G(I))
1 CONTINUE
C
C USE PHI FOR WEIGHTING FUNCTION FOR COMBINATION OF ALPHA
C AND BETA CONSTANTS AND COMBINE
C
WGHT=COSD(PHI)**2
WGHT1=1-WGHT
BETA=BET(1)*WGHT+BET(2)*WGHT1
ALPHA=ALPH(1)*WGHT+ALPH(2)*WGHT1
Q=QT(1)*WGHT+QT(2)*WGHT1
PS=PST(1)*WGHT+PST(2)*WGHT1
C
C USE THESE TO CALCULATE THETA AND PHI

```

C

```
THETA=ACOSD(COSD(ALPHA)*COSD(BETA))
IF (ALPHA .EQ. 0) THEN
  PHI=SIGN(90.,BETA)
ELSE
  PHI=ATAND(TAND(BETA)/SIND(ALPHA))
END IF
IF (ALPHA .LT. 0) PHI= PHI+180.
IF (PHI .LT. 0) PHI= PHI+360.
RETURN
END
```

```
FUNCTION POLY(V,A,B,C,D)
POLY = A + B*V + C*V*V + D*V*V*V
RETURN
END
```

References

1. Bryer, D. W.; and Pankhurst, R. C.: *Pressure-Probe Methods for Determining Wind Speed and Flow Direction*. Her Majesty's Stationery Off. (London), 1971.
2. Fearn, Richard L.; and Weston, Robert P.: *Induced Velocity Field of a Jet in a Crossflow*. NASA TP-1087, 1978.
3. Nielsen, Kaj L.: *Methods in Numerical Analysis*, Second ed. Macmillan Co., 1964.
4. Kjelgaard, Scott O.; and Sellers, William L., III: Detailed Flowfield Measurements Over a 75° Swept Delta Wing for Code Validation. Paper presented at the AGARD Symposium on Validation of Computational Fluid Dynamics (Lisbon, Portugal), May 2-5, 1988.
5. Dring, R. P.; and Suo, M.: Particle Trajectories in Swirling Flows. *J. Energy*, vol. 2, July-Aug. 1978, pp. 232-237.
6. Dring, R. P.; Caspar, J. R.; and Suo, M.: Particle Trajectories in Turbine Cascades. *J. Energy*, vol. 3, no. 3, May-June 1979, pp. 161-166.
7. Dring, R. P.: Sizing Criteria for Laser Anemometry Particles. *Trans. ASME, J. Fluids Eng.*, vol. 104, Mar. 1982, pp. 15-17.

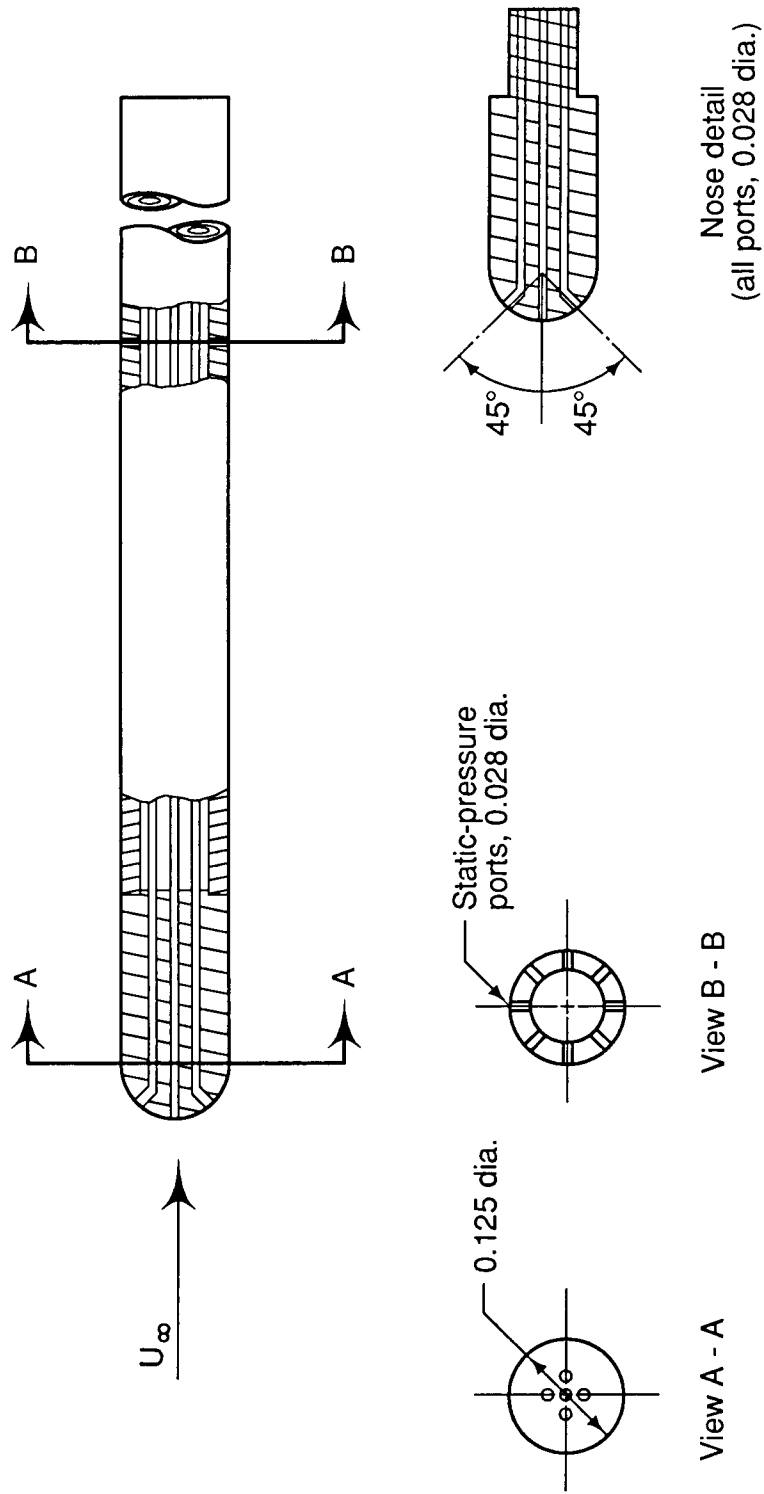


Figure 1. Details of five-hole probe. All linear dimensions are in inches.

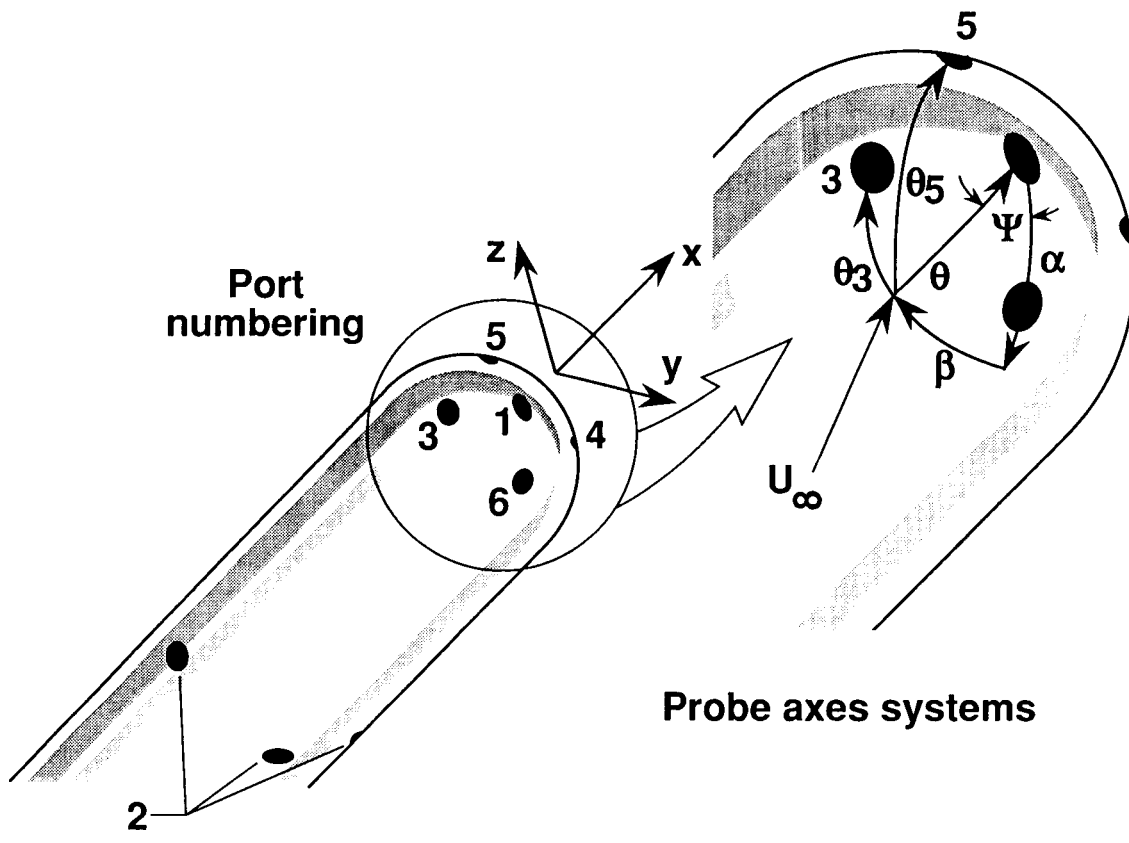


Figure 2. Coordinate system of five-hole probe.

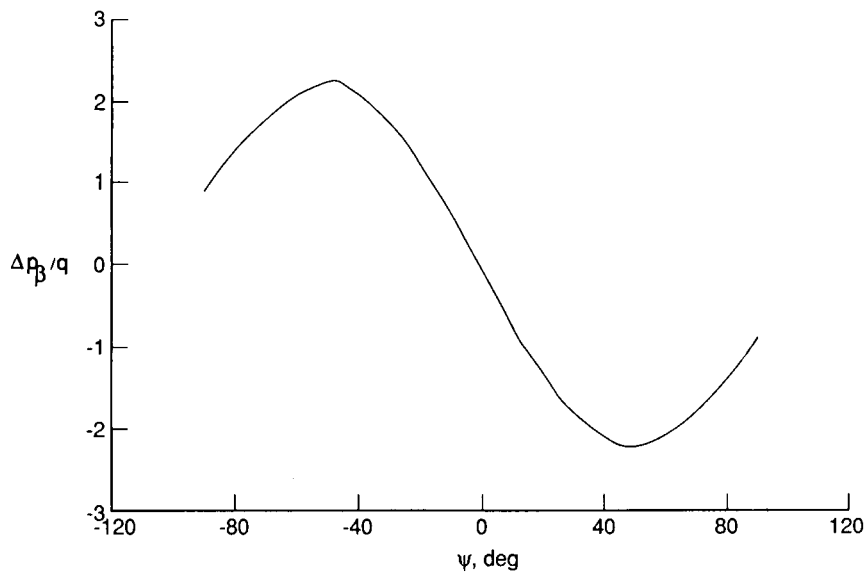
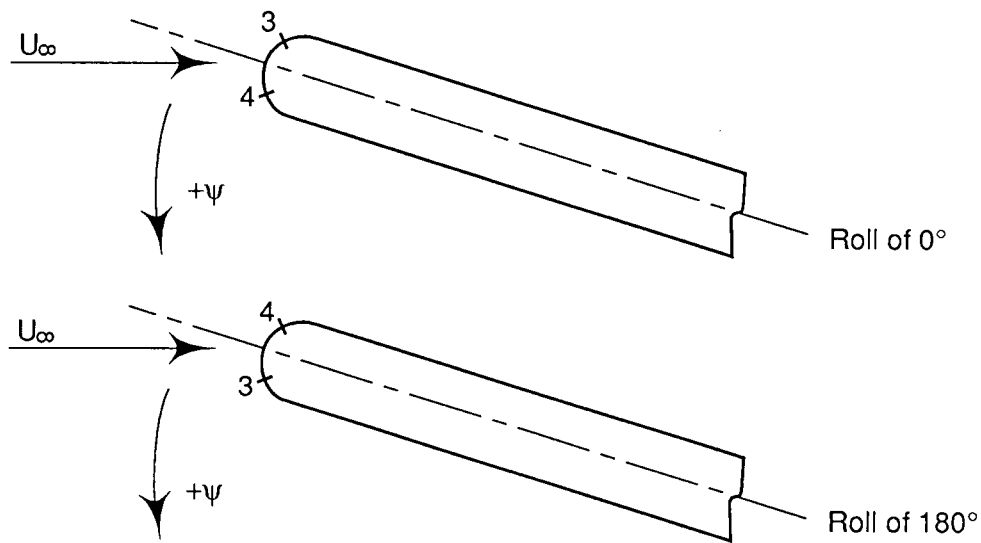
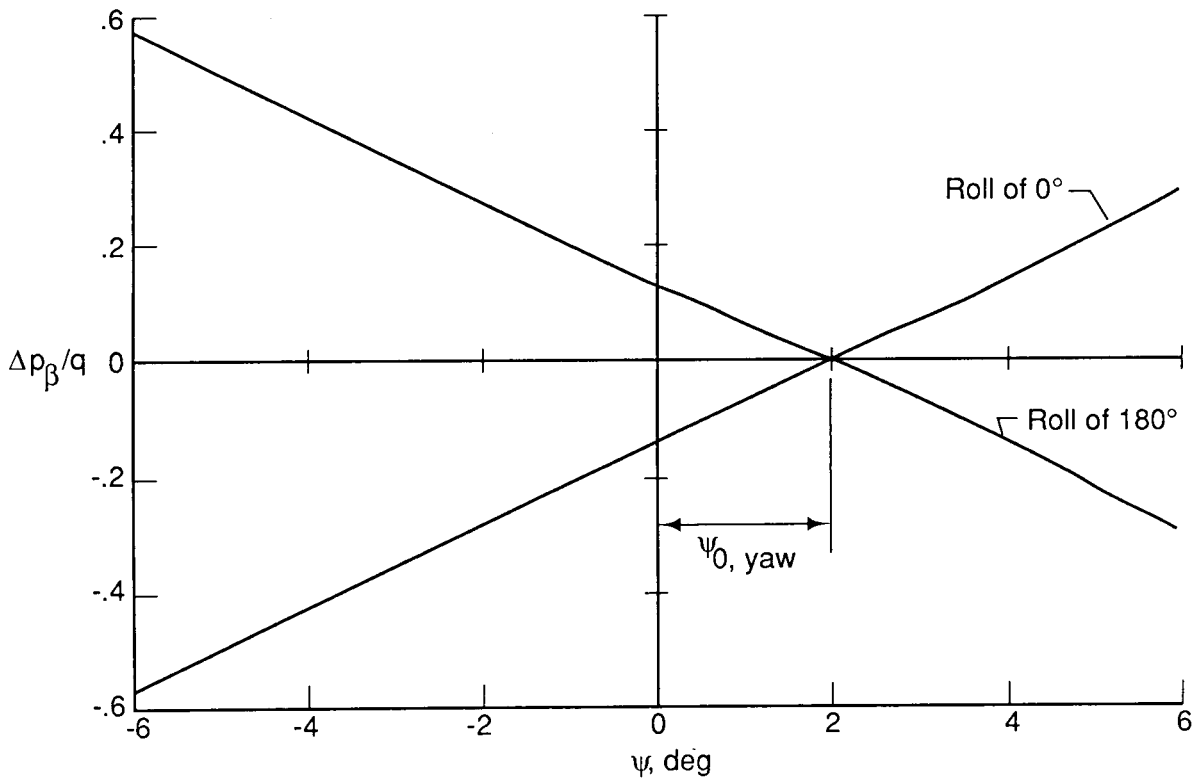


Figure 3. Typical set of calibration data.

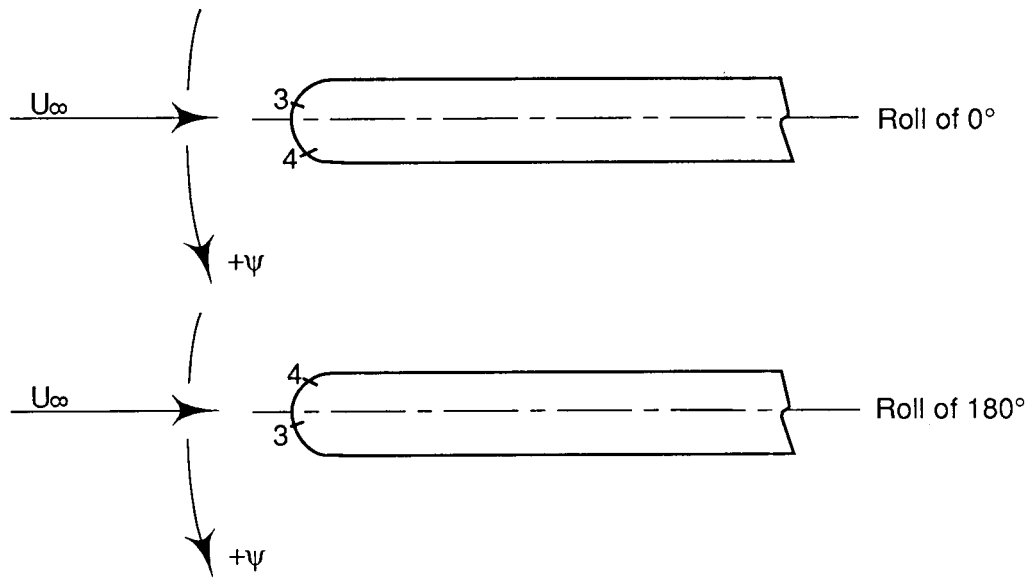


(a) Section illustrating probe misalignment with free stream. View looking down from above.

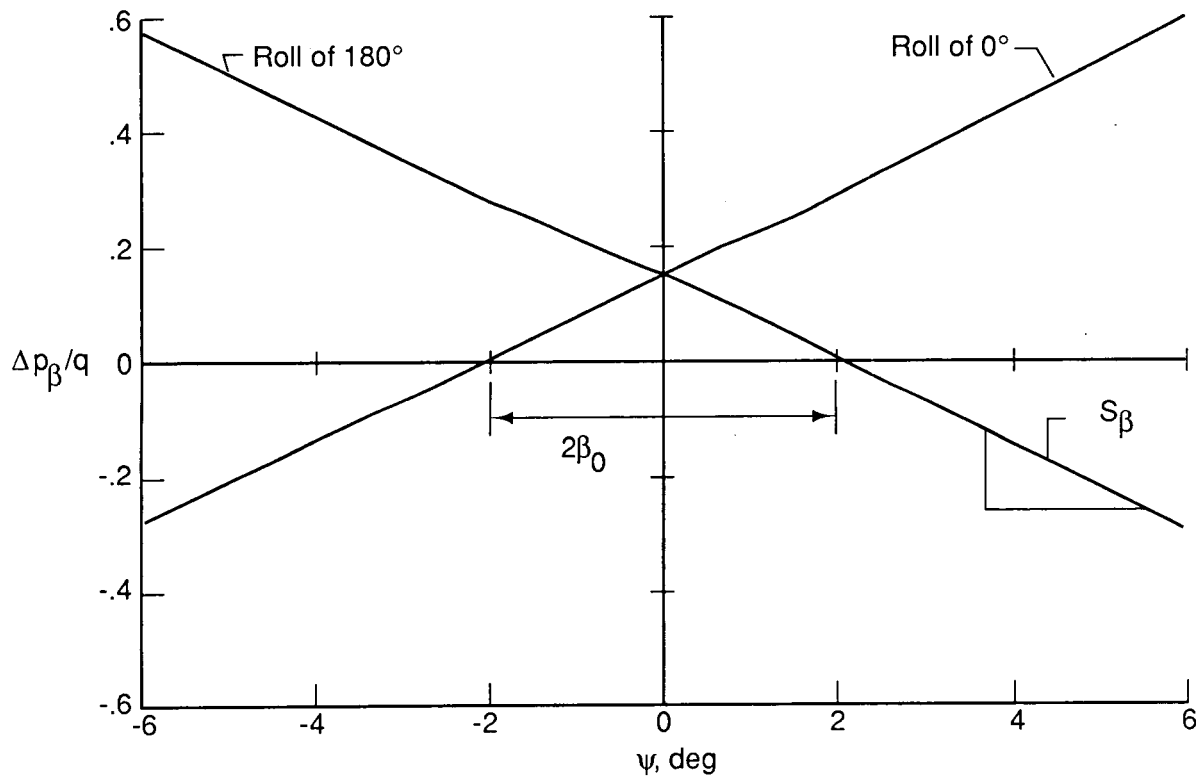


(b) Plot illustrating probe misalignment in yaw with free stream.

Figure 4. Yaw error due to misalignment with free stream.



(a) Sketch illustrating manufacturing error. View looking down from above.



(b) Plot illustrating probe manufacturing error in β ports.

Figure 5. Manufacturing error in β ports.

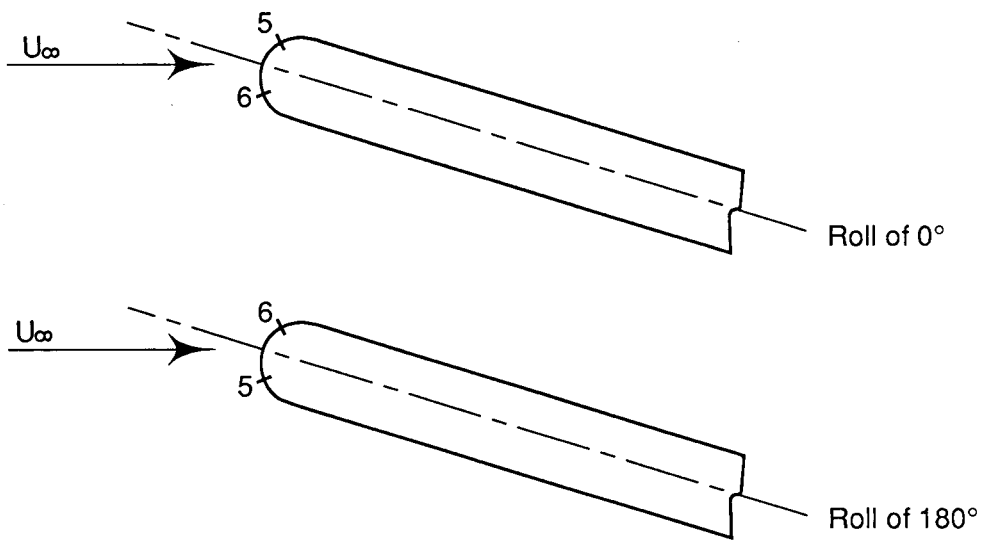


Figure 6. Sketch illustrating probe error in pitch due to misalignment with free stream. View looking from side.

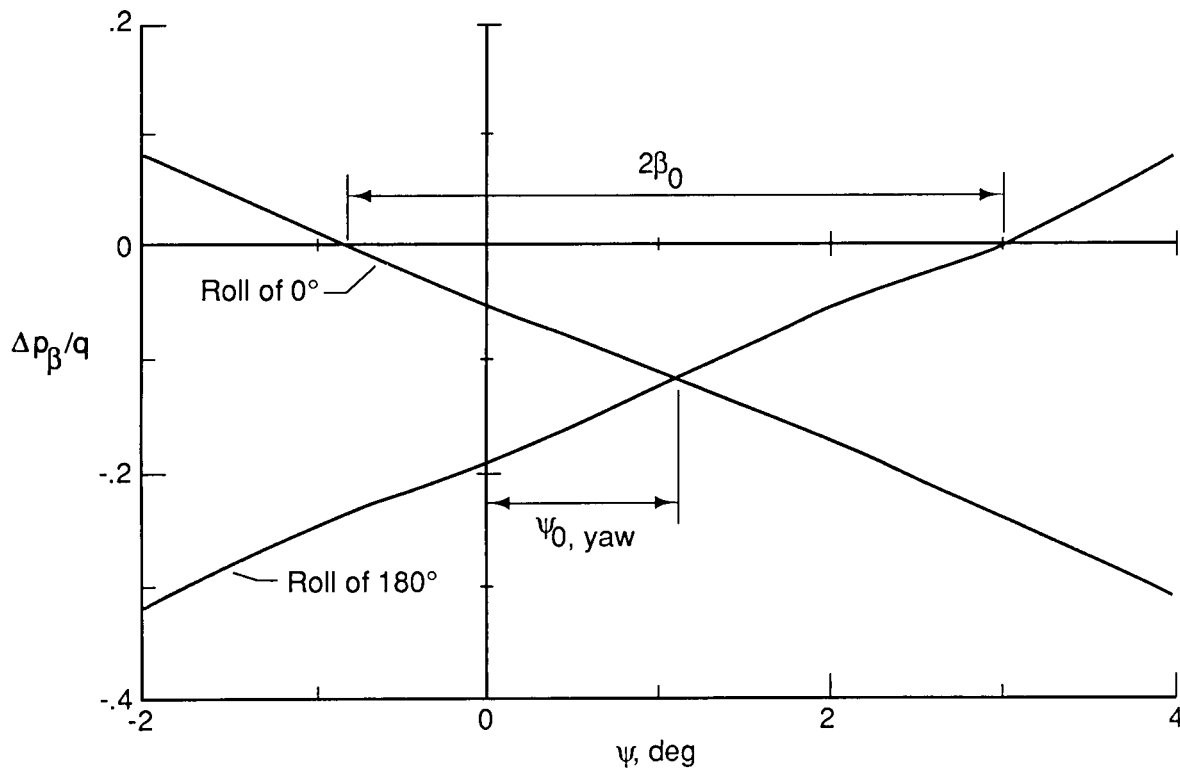
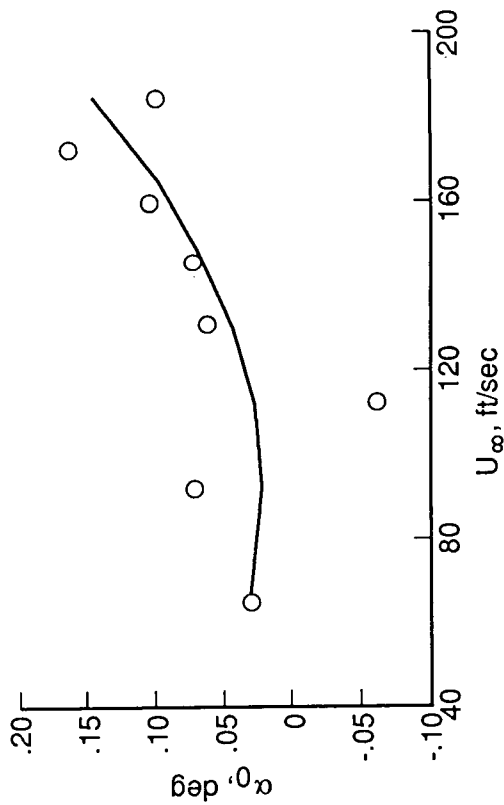
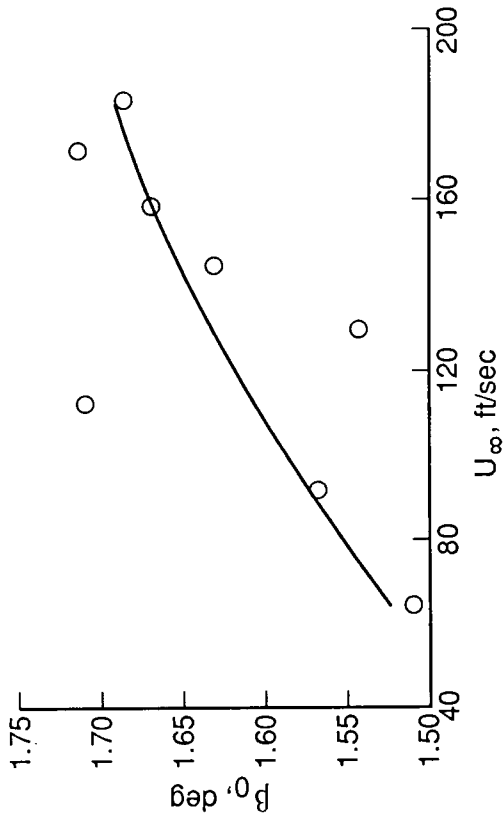


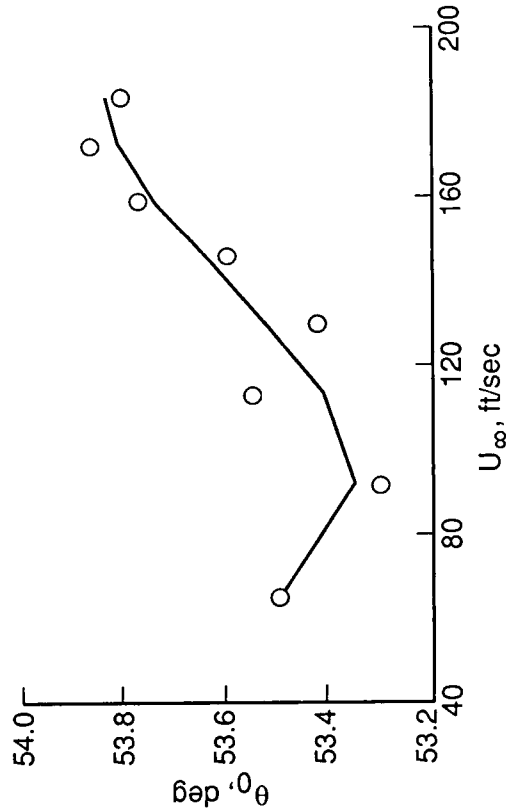
Figure 7. Typical data set presenting uncorrected calibration data.



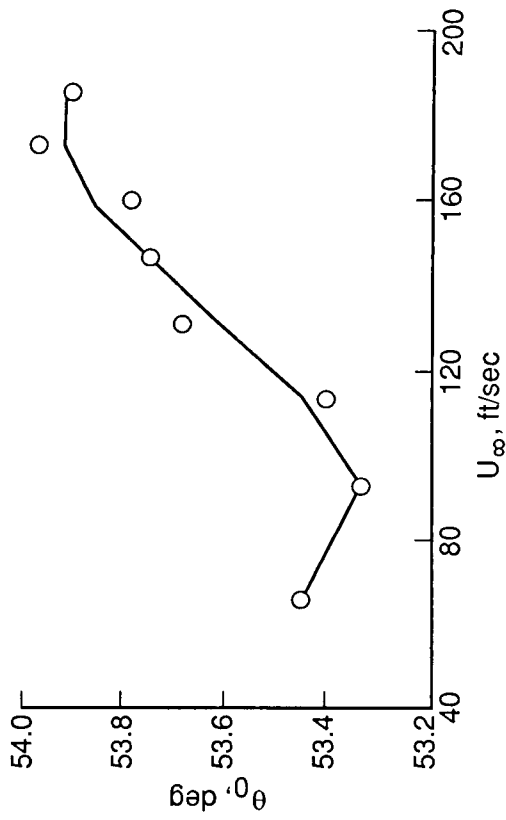
(a) α_0 versus U_∞ for rolls of 90° and 270°.



(b) β_0 versus U_∞ for rolls of 0° and 180°.

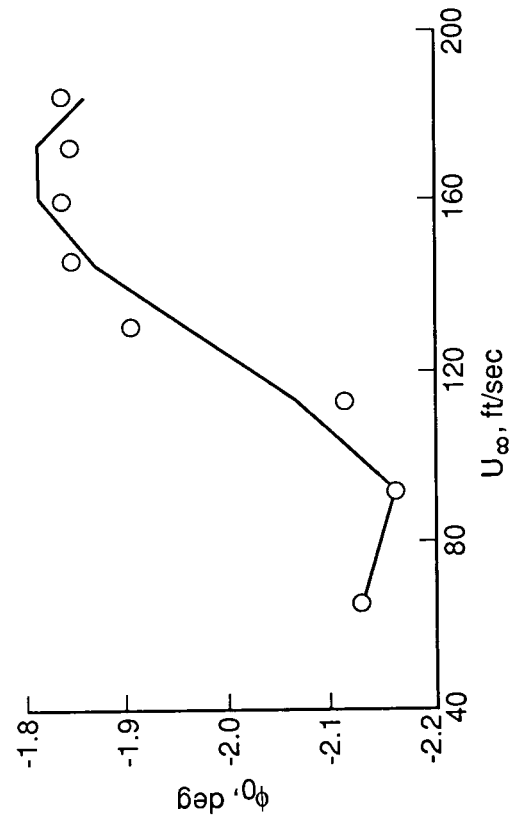


(c) θ_0 versus U_∞ for rolls of 90° and 270°.

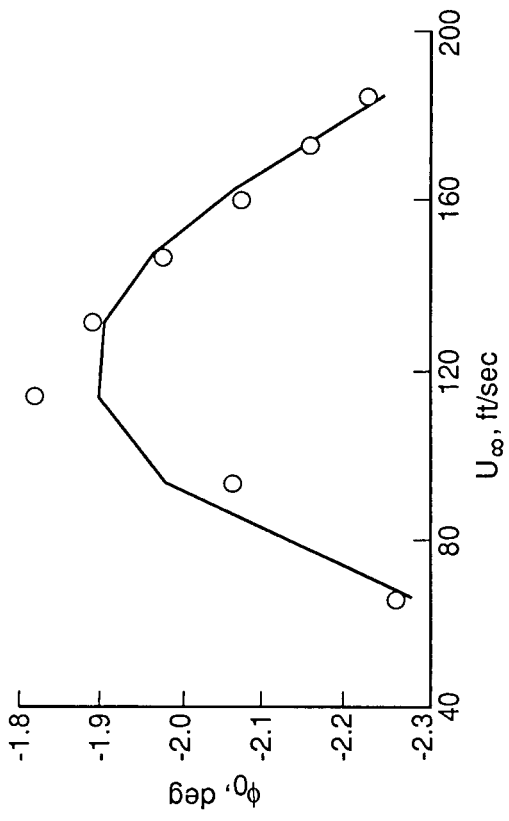


(d) θ_0 versus U_∞ for rolls of 0° and 180°.

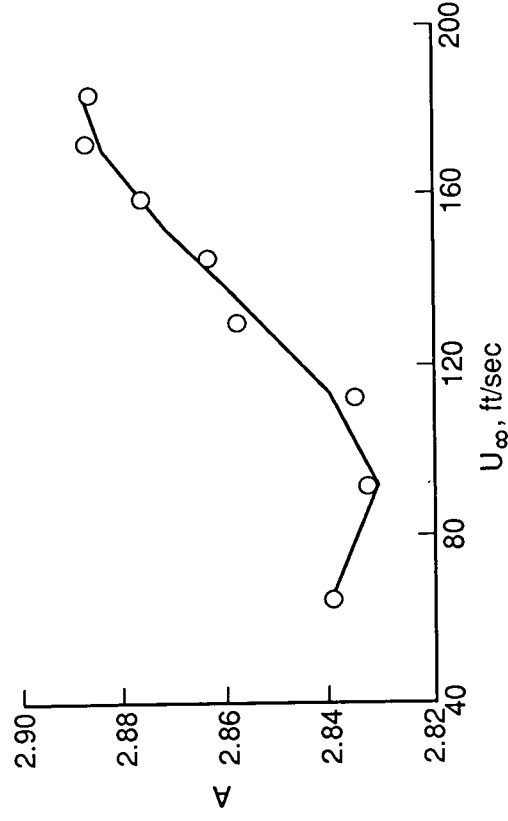
Figure 8. Variation of calibration coefficients with free-stream velocity.



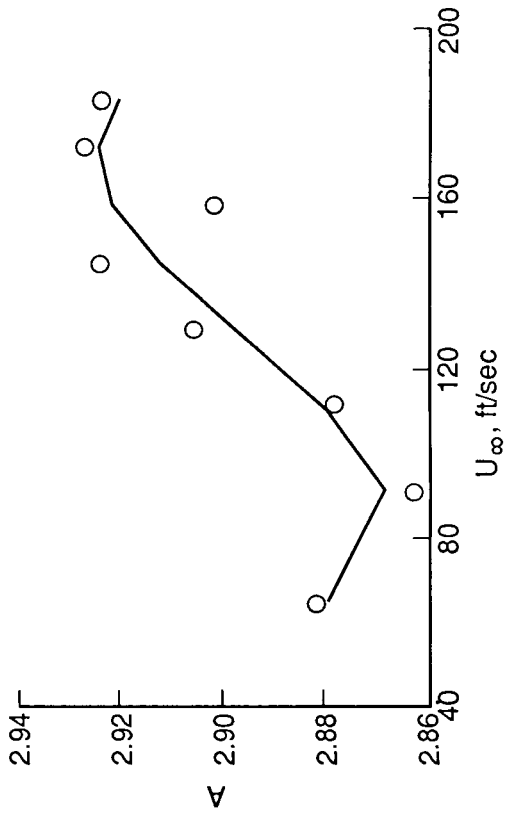
(e) ϕ_0 versus U_∞ for rolls of 90° and 270° .



(f) ϕ_0 versus U_∞ for rolls of 0° and 180° .

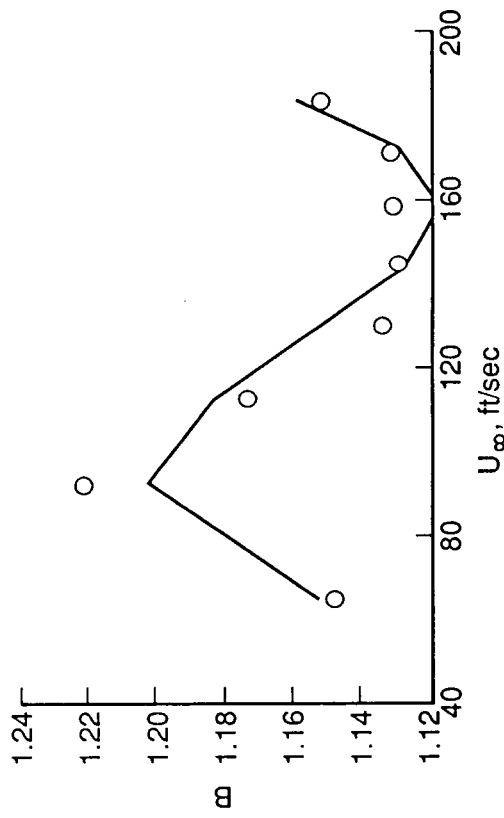


(g) A versus U_∞ for rolls of 90° and 270° .

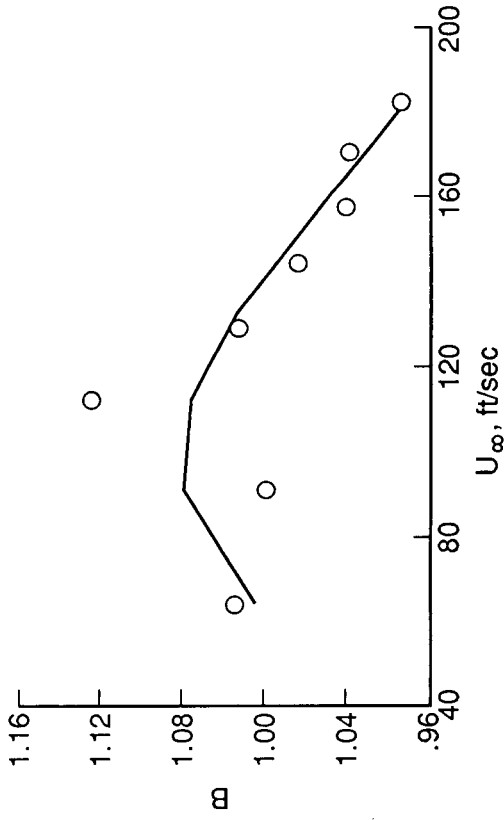


(h) A versus U_∞ for rolls of 0° and 180° .

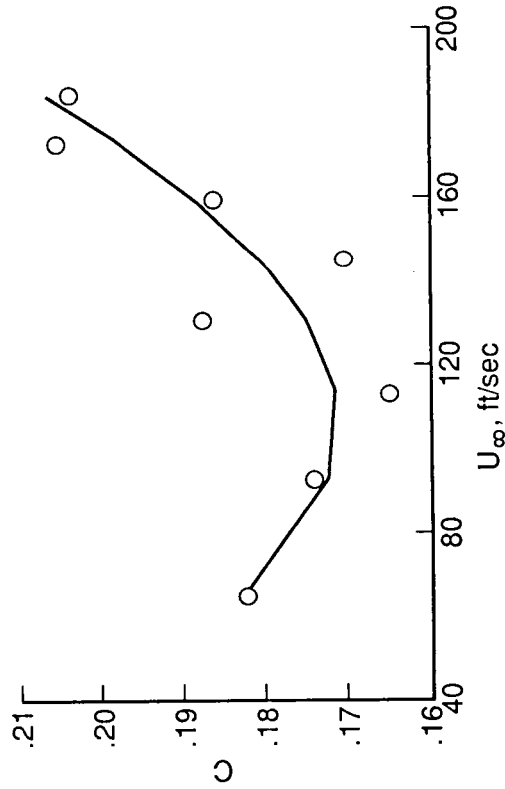
Figure 8. Continued.



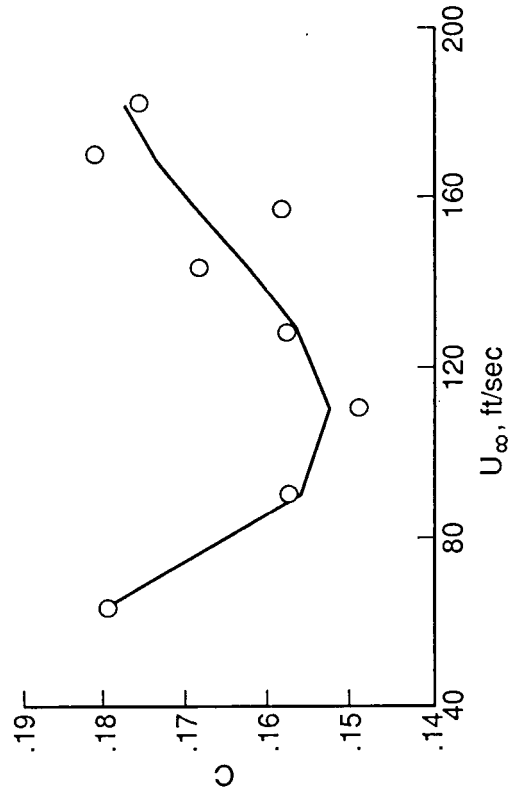
(i) B versus U_∞ for rolls of 90° and 270° .



(j) B versus U_∞ for rolls of 0° and 180° .

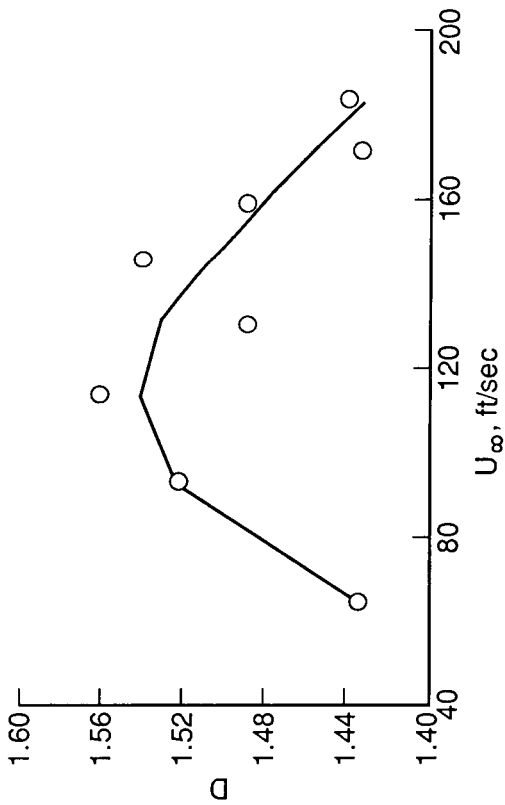


(k) C versus U_∞ for rolls of 90° and 270° .

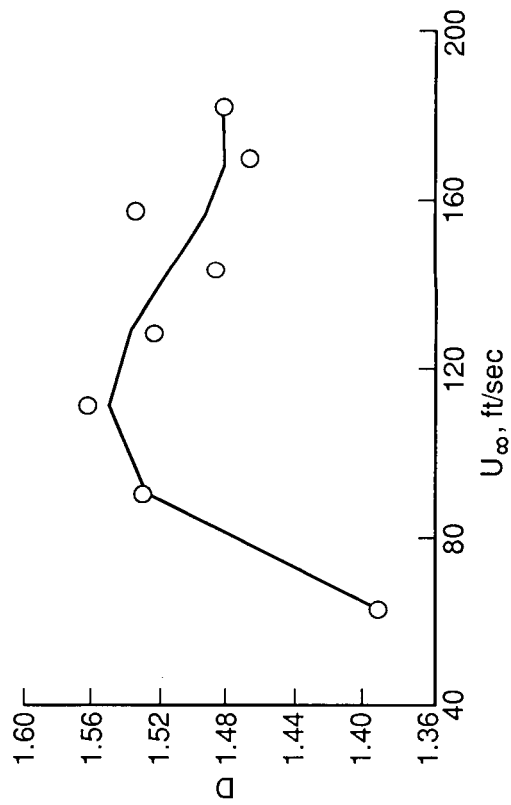


(l) C versus U_∞ for rolls of 0° and 180° .

Figure 8. Continued.



(m) D versus U_∞ for rolls of 90° and 270° .



(n) D versus U_∞ for rolls of 0° and 180° .

Figure 8. Concluded.

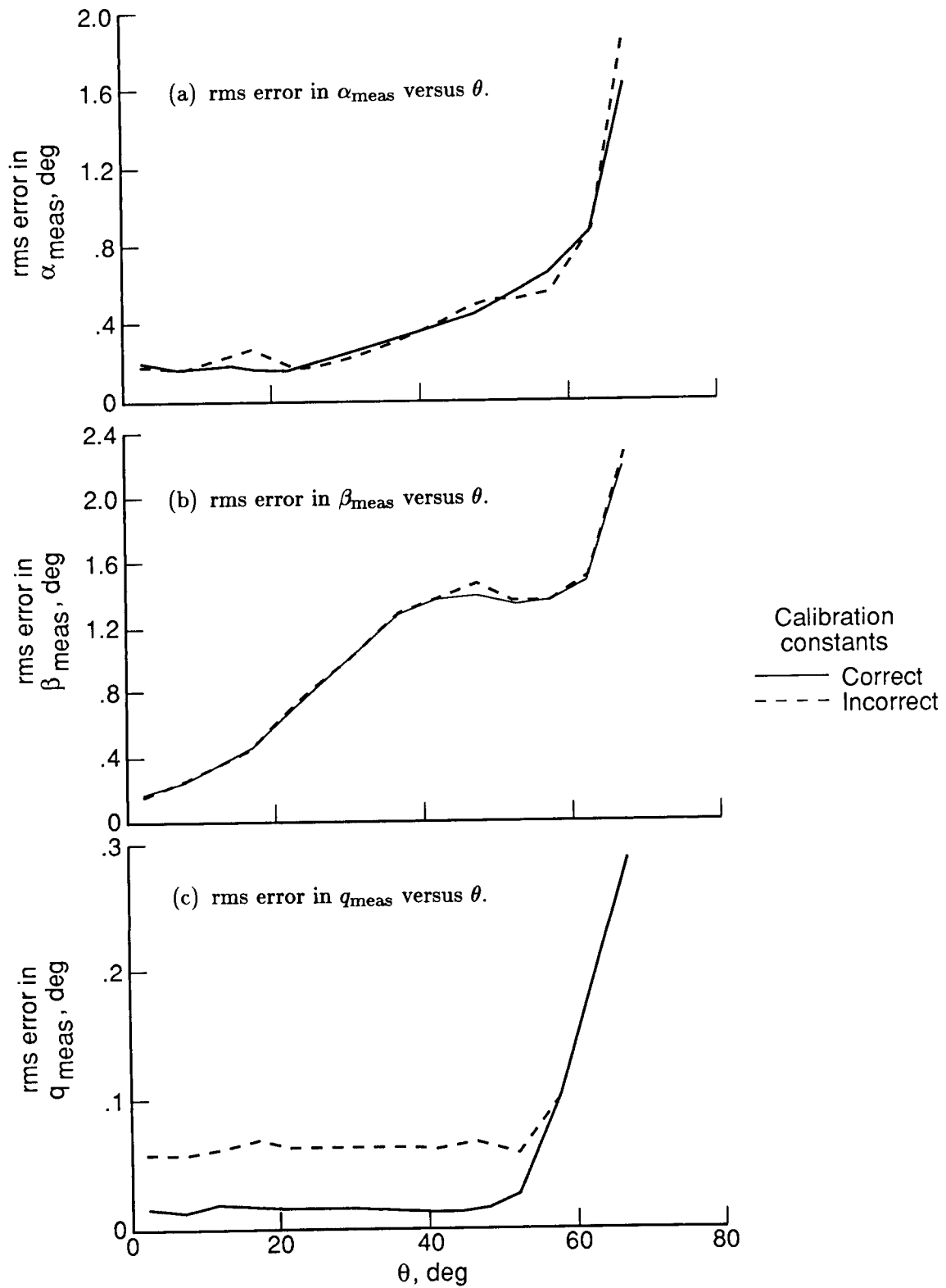
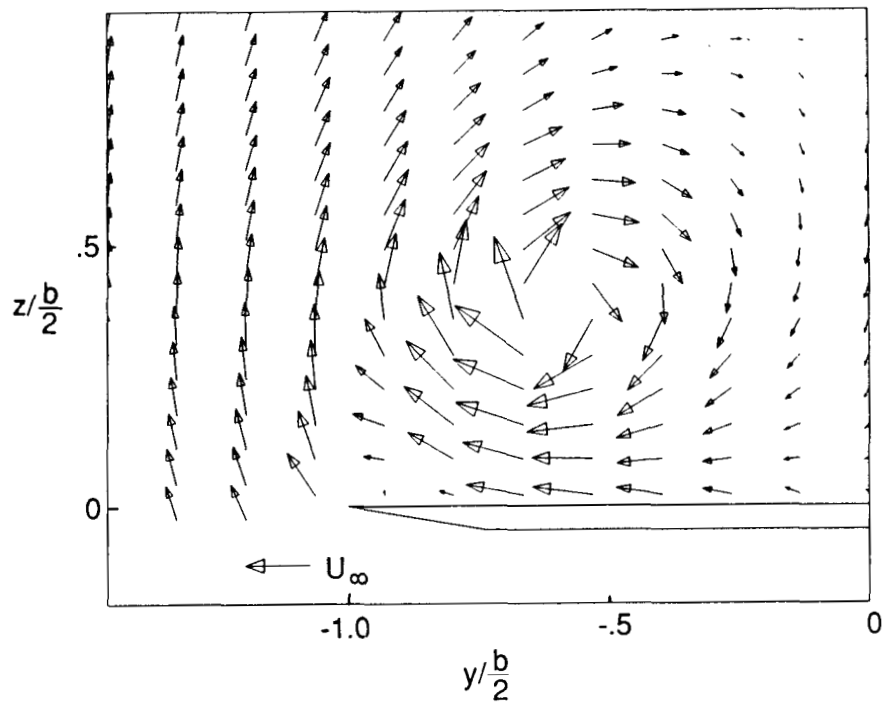
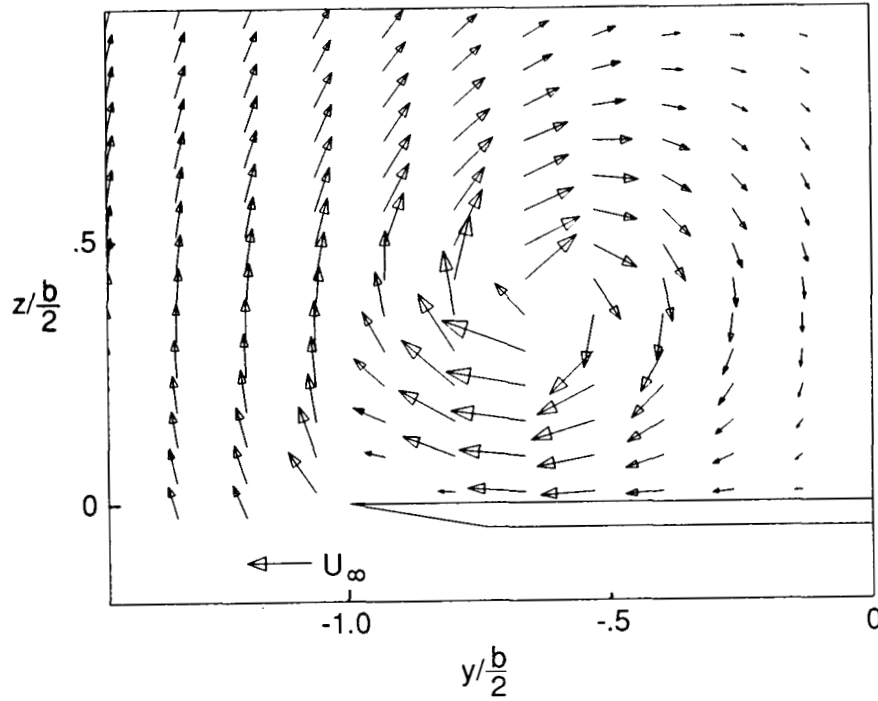


Figure 9. Characteristics of probe calibrated in this investigation.



(a) Crossflow velocity vectors measured with five-hole probe.



(b) Crossflow velocity vectors measured with three-component laser Doppler velocimeter.

Figure 10. Velocity surveys obtained over 75° -swept delta wing at an angle of attack of 20.5° , $x/L = 0.9$, and $R = 1 \times 10^6$.

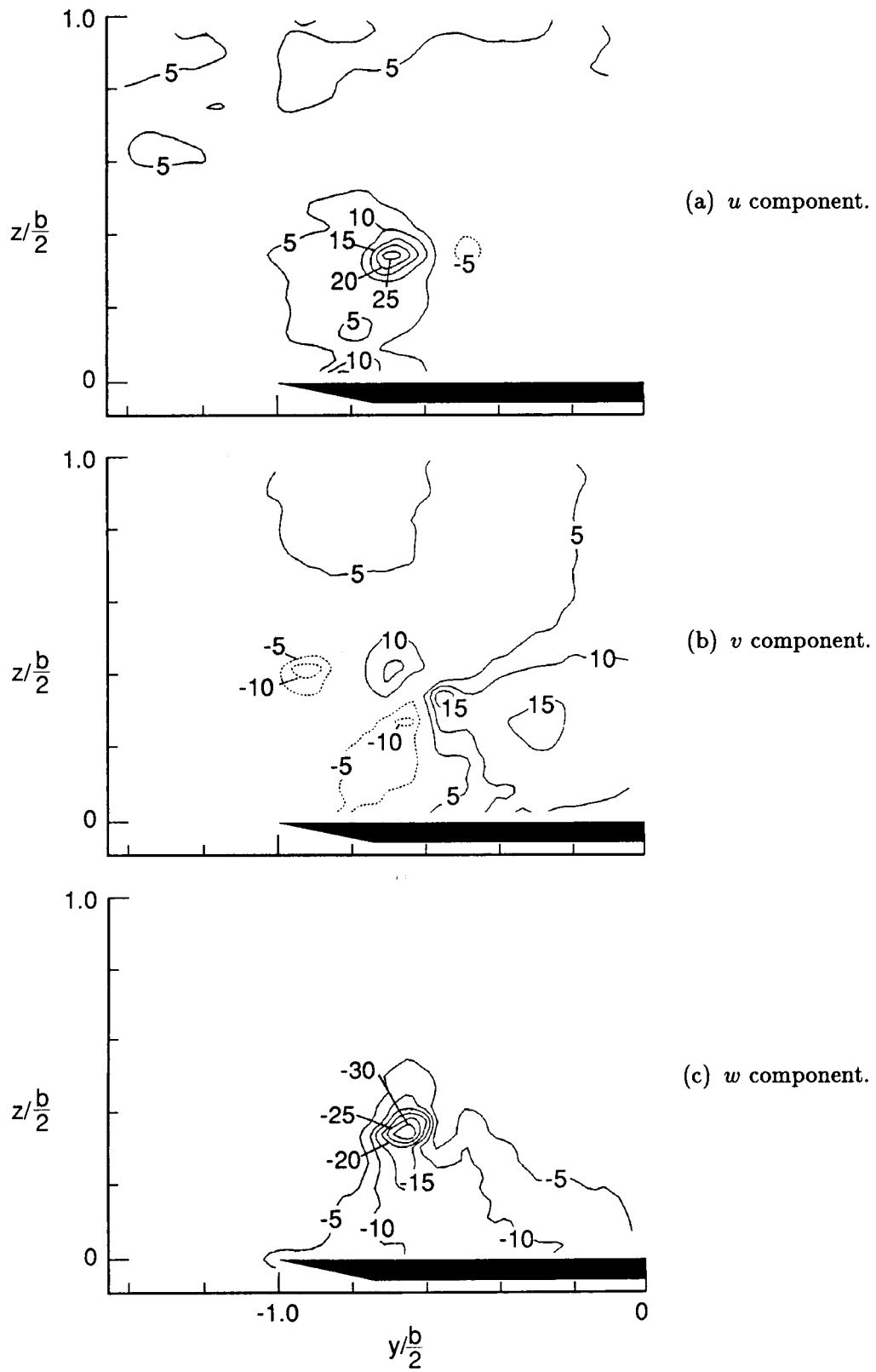


Figure 11. Differences in measured velocities between LDV and five-hole probe. $x/L = 0.9$; $R = 1 \times 10^6$.



Report Documentation Page

1. Report No. NASA TM-4047	2. Government Accession No.	3. Recipient's Catalog No.	
4. Title and Subtitle Theoretical Derivation and Calibration Technique of a Hemispherical-Tipped, Five-Hole Probe		5. Report Date December 1988	
		6. Performing Organization Code	
7. Author(s) Scott O. Kjelgaard		8. Performing Organization Report No. L-16454	
		10. Work Unit No. 505-60-11-03	
9. Performing Organization Name and Address NASA Langley Research Center Hampton, VA 23665-5225		11. Contract or Grant No.	
		13. Type of Report and Period Covered Technical Memorandum	
12. Sponsoring Agency Name and Address National Aeronautics and Space Administration Washington, DC 20546-0001		14. Sponsoring Agency Code	
		15. Supplementary Notes	
16. Abstract A technique is presented for the calibration of a hemispherical-tipped, five-hole probe having a 0.125-in. diameter. Equations are derived from the potential flow over a sphere relating the flow angle and velocity to pressure differentials measured by the probe. The technique for acquiring the calibration data and the technique for calculating the calibration coefficients are presented. The accuracy of the probe in both the uniform calibration flow field and the nonuniform flow field over a 75°-swept delta wing is discussed.			
17. Key Words (Suggested by Authors(s)) Pressure probe Yaw-pitch probe Five-hole probe Probe calibration		18. Distribution Statement Unclassified—Unlimited Subject Category 02	
19. Security Classif.(of this report) Unclassified	20. Security Classif.(of this page) Unclassified	21. No. of Pages 25	22. Price A02